Enhancing Fine-Tuning Free Clinical Reasoning via Test-Time Scaling

Ji Young Byun
Johns Hopkins University

Young-Jin Park
Massachusetts Institute of Technology

Navid Azizan
Massachusetts Institute of Technology

Rama Chellappa
Johns Hopkins University

Abstract

As a cornerstone of modern healthcare, artificial intelligence is expected to support diverse medical tasks, with large language models (LLMs) offering a promising path to enhanced capabilities. Although LLMs have demonstrated solid performance in text-based tasks, their application in medical imaging, particularly for reasoning-based diagnosis, remains largely unexplored. This gap is further exacerbated by the impracticality of supervised fine-tuning for clinical reasoning tasks, owing to limited data availability and high annotation costs. In this work, we introduce a fine-tuning–free framework for medical image diagnosis that enhances reasoning through test-time scaling (TTS). Our approach operates in two stages: given either visual or textual inputs, candidate representations or reasoning steps are first generated, and then aggregated through a self-consistency decoding strategy to yield robust final predictions. This framework avoids the need for expensive supervision while leveraging additional inference-time computation to improve reliability. We provide both a theoretical analysis—deriving scaling laws that characterize when and how TTS yields reliable gains—and a comprehensive empirical evaluation across medical benchmarks spanning both textual and visual modalities. Results demonstrate consistent improvements over single-pass inference baselines, with performance gains of up to 30.4 percentage points, highlighting the potential of TTS as a practical pathway toward trustworthy medical reasoning without specialized reward models or domain-specific fine-tuning.

1. Introduction

Large language models (LLMs) and vision-language models (VLMs) have shown strong performance across diverse domains, including mathematics [25], robotics [14], autonomous driving [20], and scientific research [22, 35]. A central factor in these advances is their ability to perform *reasoning*. While conventional deep learning models are often treated as black-box predictors that output final classifications without rationale, recent reasoning language models (RLMs) can articulate intermediate steps that explain how answers are derived.

In medicine, where decisions are safety-critical, transparent reasoning is particularly important. Beyond predicting class probabilities, models should justify their decisions in alignment with clinical workflows, and their outputs should be evaluated to mitigate risks of deviating from clinical standards [10]. To address these requirements, recent studies have investigated vision-language models (VLMs), which can generate intermediate reasoning in natural language. In particular, VLMs have been applied to medical image diagnosis, commonly referred as visual question answering (VQA) [13, 18, 29].

Explicit multi-step reasoning methods, such as chain-of-thought (CoT) prompting [27, 34], produce step-by-step explanations that enhance problem-solving ability. These approaches have proven effective in domains such as arithmetic and symbolic reasoning, but their use in medicine remains limited. Multi-stage reasoning aligns naturally with clinical practice, where clinicians sequentially observe, interpret, and diagnose. Early studies have applied CoT-style prompting to medical tasks [16, 30], allowing models to explore multiple hypotheses before reaching a conclusion.

However, the effectiveness of multi-stage reasoning often depends on fine-tuning with large collections of annotated reasoning processes. In medicine, such annotations require domain experts and are costly to obtain. This scarcity motivates approaches that *do not rely on fine-tuning*, including zero-shot methods, which are promising for extending reasoning-capable language models (LMs) to medical domains without extensive supervision.

Zero-shot prediction with LMs, however, often yields suboptimal performance. To address this, *test-time scaling* (TTS) has recently emerged as a promising inference paradigm. The key idea is to allocate additional computation during inference to improve a model's reasoning abil-

ity. A common strategy is "parallel thinking", where multiple candidate outputs are sampled and aggregated, rather than relying on a single generated output (i.e., single-pass decoding) [25, 38]. These approaches, ranging from majority voting [33] to verifier-based selection [4, 15, 31, 32], have demonstrated strong performance in domains requiring complex reasoning, such as mathematics.

Directly transferring TTS methods, particularly those leveraging verifiers, to medical applications presents significant challenges. Verifiers, also known as reward models, are often unavailable in the medical domain because their training requires vast amounts of labeled reward data. For example, Qwen-PRM [39]—a reward model used for mathematical reasoning—required 4.5 million labels for its training. Consequently, TTS methods in the medical setting have largely focused on reward-free inference schemes, such as self-consistency decoding [24], mostly on textual benchmarks.

Despite these efforts, our understanding of TTS in medicine remains limited. Key open questions include: **under what conditions does TTS improve performance?** and **can these methods extend beyond text to multimodal medical VQA tasks?** Motivated by these limitations, this work presents a simple yet effective fine-tuning free framework that integrates a TTS strategy to enhance clinical reasoning and support reliable medical diagnosis, without requiring additional supervision or a specialized reward model.

Our key contributions are summarized as follows:

1. *Framework.* We investigate inference strategies (direct answering and CoT) and introduce a two-stage reasoning framework for medical VQA, where a VLM produces textual descriptions that are aggregated by an LLM for diagnosis.
2. *Theoretical Analysis.* We provide a formal analysis of TTS, deriving scaling laws that characterize how performance improves with the number of samples and identifying conditions under which TTS yields reliable gains.
3. *Empirical Validation.* We evaluate TTS on test-time inference strategies and show consistent improvements, with gains of up to 30.4 percentage points over single-pass baselines.

A detailed discussion of related work is in the Appendix A.

2. Methods

This paper presents an approach to modality-agnostic medical question answering (QA), with the goal is to generating accurate answers to clinically relevant questions based on given input data without requiring task-specific fine-tuning. Formally, a medical QA problem can be represented as a triplet $(\boldsymbol{x}, q, y)$, where:

- $\boldsymbol{x}$ denotes the *context*, which may take different modalities.
- q represents the *problem description*, expressed as a natural language query about the context.
- y is the *ground truth answer*, serving as the target output for the model.

For example, in a medical visual QA (VQA) setting, the context $\boldsymbol{x}$ may correspond to a chest X-ray. The query q would be a natural language prompt, such as "Does this patient have pneumonia?", while the ground truth answer y is a categorical label (e.g., 0 – normal, 1 – pneumonia).

This formalization provides a unified framework that accomodates a broad spectrum of medical QA tasks, ranging from text-based multiple choice to image-based VQA tasks.

2.1. Test-Time Inference Strategies

Owing to the versatility of reasoning language models, medical QA problems can be addressed through multiple inference paradigms. In this section, we describe two widely adopted strategies—zero-shot and CoT reasoning—that are broadly utilized across medical QA tasks. We further introduce a two-stage reasoning framework, illustrated in Figure 1, which is specifically designed for medical VQA. While zero-shot and CoT methods yield an answer within a single inference step, our two-stage reasoning framework explicitly decomposes the process into two distinct phases.

2.1.1. Direct Answering

Consider a language model (LM), such as Llama 3.2-Vision instruction-tuned model, that takes a textual prompt q and a context $\boldsymbol{x}$ and produces an answer a. A straightforward way to use such a model for diagnosis is to directly request a prediction of the target categorical label. For instance, we can set $q \leftarrow$ "`Given a pediatric chest X-ray image, classify it as 0 (normal) or 1 (pneumonia).`" The model directly provides a final answer without requiring any reasoning. We refer to this as the *Direct Answering* method.

2.1.2. Chain-of-Thought (CoT) Prompting

An alternative is to prompt the model to provide a step-by-step explanation before giving the final answer. This can be done by adding a phrase such as "`Let's think step by step.`" before the answer prompt [11]. This method, commonly called chain-of-thought (CoT), encourages the model to reveal its reasoning process rather than just providing the final classification. We denote this approach as *one-stage CoT* method.

2.1.3. Two-Stage Reasoning for VQA

According to recent theoretical and experimental evidence [1], the Transformer architecture often benefits when a complex task is decomposed into simpler sub-tasks. Motivated by this observation, we propose *describe-then-diagnose*, a two-stage approach to help the Transformer arrive at a more

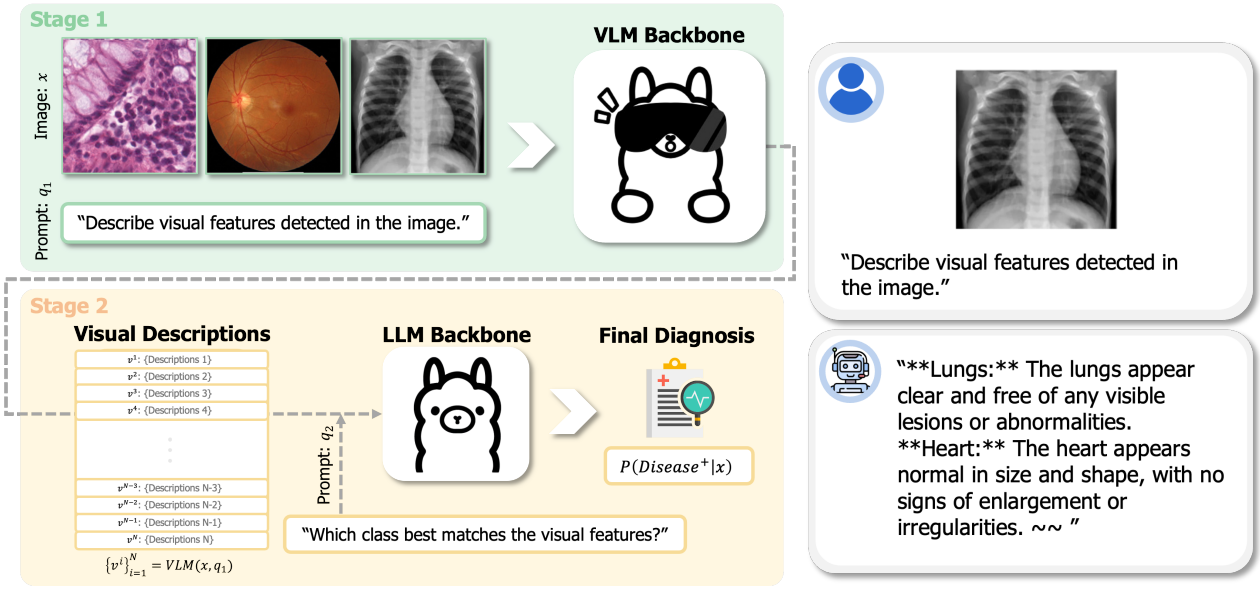

(a) (b)

Figure 1. Graphical illustration of our proposed test-time-scaled reasoning framework for reliable zero-shot medical image diagnosis. Panel (a) details Stage 1, in which the VLM receives an image and a text prompt to generate N visual description samples, with Stage 2 applying a test-time scaling technique to determine the final diagnostic probability. Panel (b) shows a representative example of a healthy subject's chest X-ray paired with textual prompt and one of the N generated visual descriptions from VLM in Stage 1.

accurate diagnosis in a VQA setting and test-time compute scaling friendly.

Visual Description Generation. We first instruct the VLM to generate descriptions on visual features of the input image without directly querying for a diagnosis, illustrated in Figure 1b. Concretely, we prompt the VLM as follows: $v = \mathsf{VLM}(\boldsymbol{x}, q_1)$ where q_1 can be `"Describe visual features detected in the image"`.

Diagnosis from Descriptions. The generated visual descriptions v is then provided as input to a (potentially different) LLM that produces a final diagnosis. For example, we can construct the query: $q_2(v)$:= "`Decide which class best matches the visual features described: 0 (normal) or 1 (pneumonia). **Features:** {features}`", where we substitute `{features}` with the previously generated v. Then, the diagnosis is obtained via:

$$a = \mathsf{LLM}(q_2(v)) = \underbrace{\mathsf{LLM}\Big(q_2\Big(\underbrace{\mathsf{VLM}(\boldsymbol{x}, q_1)}_{\text{Describe}}\Big)\Big)}_{\text{Diagnose}} \quad (1)$$

2.2. Enhanced Clinical Reasoning via Scaling Test-Time Compute

As we will demonstrate later, general-purpose reasoning language models such as LLAMA or DEEPSEEK often struggle to provide accurate answers in medical QA settings. While this limitation could in principle be alleviated through finetuning, the high cost of clinical experts' time and the inherent complexity of medical decision-making make large-scale data annotation prohibitively expensive and scarce. To overcome this challenge, we comprehensively investigate the applicability of test-time scaling techniques—recently introduced in the context of mathematical reasoning tasks [25, 38]—to the domain of medical QA. In particular, we adopt self-consistency decoding [33] for our application, given the absence of reliable reward models in the medical domain.

One-Stage TTS. We estimate class probabilities by sampling N independent outputs from a (reasoning) language model LM under randomized decoding (e.g., temperature scaling [6]). Let the label space be $\mathcal{Y} = \{1, \ldots, C\}$. For each draw $i \in \{1, \ldots, N\}$, the model produces an answer string $a^{(i)}$, which we map to a class via a parseϕ : text$\to\mathcal{Y}$ (e.g., extracting "A/B/C/D" or $\{1, \ldots, C\}$). Denote the parsed class by $\hat{a}^{(i)} = \phi(a^{(i)}) \in \mathcal{Y}$. Formally,

$$\{a^{(i)}\}_{i=1}^{N} \overset{\text{i.i.d.}}{\sim} \mathsf{LM}(\boldsymbol{x}, q), \qquad \hat{y}^{(i)} = \phi(a^{(i)}). \quad (2)$$

Each $\hat{y}^{(i)}$ can be viewed as a draw from the LM-induced predictive distribution over classes, $p(y \mid \boldsymbol{x}, q)$. We estimate these class probabilities by Monte Carlo:

$$\widehat{p}(y = c \mid \boldsymbol{x}, q) \;=\; \frac{1}{N} \sum_{i=1}^{N} \mathbb{I}(\hat{y}^{(i)} = c). \quad (3)$$

The final prediction is the maximum-probability class under this estimate:

$$\hat{y} \;=\; \arg \max_{c \in \{1,\dots,C\}} \widehat{p}(y = c \mid \boldsymbol{x}, q). \quad (4)$$

Two-Stage TTS. In a two-stage inference framework, we can apply TTS both in the description stage and in the diagnosis stage. Formally,

$$\{v^{(i)}\}_{i=1}^{N} \overset{\text{i.i.d.}}{\sim} \mathsf{VLM}(\boldsymbol{x}, q_1) \quad (5)$$

$$\{a^{(i,j)}\}_{j=1}^{M} \overset{\text{i.i.d.}}{\sim} \mathsf{LM}(v^{(i)}, q_2). \quad (6)$$

where $v^{(i)}$ denotes the i-th description sampled from the vision–language model in the first stage, and $a^{(i,j)}$ is the j-th diagnosis generated by the language model given that description in the second stage.

Empirically, we observe that even under randomized decoding, the diagnosis $a^{(i,j)}$ remains unchanged for a fixed description $v^{(i)}$. This indicates that *the predictive uncertainty originates from the reasoning process (description stage) rather than from the decision-making process (diagnosis stage)*. Consequently, there is no measurable gain from scaling test-time compute in the second stage, and we therefore set $M = 1$. The final class probabilities and prediction are then estimated in the same way as in the single-stage case.

2.3. When Does TTS Help? A Formal Analysis

While self-consistency decoding has demonstrated strong empirical performance in both medical applications [23, 24] and mathematical reasoning tasks [2], it remains underexplored whether TTS can be broadly applied across different large language models and how its scaling behavior unfolds (e.g., whether it converges quickly or grows monotonically). To address this gap, we first present a theoretical analysis of TTS based on self-consistency decoding. Proofs are in the Appendix B.

Setup. Consider C-class classification with true class $c^\star$. A single decode (vote) from the LM yields label $y \in \{1, \dots, C\}$ with

$$\mathbb{P}(y = c^\star) = p, \qquad \mathbb{P}(y = j) = p_j \;\; (j \neq c^\star) \quad (7)$$

where $p + \sum_{j \neq c^\star} p_j = 1$. We draw N i.i.d. votes, let X_j be the number of votes for class j, and predict by majority vote $\hat{y}_{\mathrm{MV}} = \arg\max_j X_j$ (break ties uniformly at random). Define the strongest competitor $q := \max_{j \neq c^\star} p_j$.

Proposition 1 (Majority vote vs. strongest competitor)**.** *If $p > q$, then*

$$\mathbb{P}(\hat{y}_{\mathrm{MV}} \neq c^\star) \;\leq\; (C-1)\, \exp\Big(-\frac{N}{2}\,(p-q)^2\Big), \quad (8)$$

so the error decays exponentially in N, and improves as the margin $p - q$ grows (i.e., LM becomes more confident).

Conversely, if $q > p$, then

$$\mathbb{P}(\hat{y}_{\mathrm{MV}} = c^\star) \;\leq\; (C-1)\, \exp\Big(-\frac{N}{2}\,(q-p)^2\Big), \quad (9)$$

so $\hat{y}_{\mathrm{MV}}$ amplifies the wrong class as N grows.

Corollary 1 (Exponential scaling)**.** *If $p > q$, the error of $\hat{y}_{\mathrm{MV}}$ decays exponentially with N, and to achieve $\mathbb{P}(\hat{y}_{\mathrm{MV}} \neq c^\star) \leq \delta$ it suffices that*

$$N \;\geq\; \frac{2}{(p-q)^2}\, \log\Big(\frac{C-1}{\delta}\Big). \quad (10)$$

If $q > p$, then $\mathbb{P}(\hat{y}_{\mathrm{MV}} = c^\star)$ decays exponentially in N at the same rate.

Proposition 2 (Symmetric distractors)**.** *Assume the wrong-class mass is uniform: $p_j = q_0 := \frac{1-p}{C-1}$ for all $j \neq c^\star$. Let $\{y_j\}_{j \neq c^*} \overset{\text{i.i.d.}}{\sim} \mathrm{Binomial}(N, q_0)$ be i.i.d. upper bounds for the wrong-class counts. For any threshold $t \in (0, N)$,*

$$\mathbb{P}(\hat{y}_{\mathrm{MV}} = c^\star) \;\geq\; 1 - \underbrace{\mathbb{P}(\mathrm{Bin}(N,p) \leq t)}_{\text{true class too small}} - \underbrace{\mathbb{P}(\max_{j \neq c^\star} y_j \geq t)}_{\text{some distractor too large}}. \quad (11)$$

In particular, with $t = \frac{N}{2}$,

$$\mathbb{P}(\hat{y}_{\mathrm{MV}} = c^\star) \;\geq\; \sum_{k=\lfloor N/2 \rfloor + 1}^{N} \binom{N}{k} p^k (1-p)^{N-k}. \quad (12)$$

Proposition 3 (Worst-case single distractor)**.** *Assume $p_{j^\dagger} = 1 - p$ for some $j^\dagger \neq c^\star$ and $p_j = 0$ otherwise. Then*

$$\mathbb{P}(\hat{y}_{\mathrm{MV}} = c^\star) = \sum_{k=\lfloor N/2 \rfloor + 1}^{N} \binom{N}{k} p^k (1-p)^{N-k} + \frac{1}{2}\, \mathbf{1}_{\{N \text{ even}\}} \binom{N}{N/2} p^{N/2} (1-p)^{N/2}. \quad (13)$$

In particular, the majority vote strictly helps over single-pass iff $p > 1/2$, and

$$\mathbb{P}(\hat{y}_{\mathrm{MV}} \neq c^\star) = \mathbb{P}(\mathrm{Bin}(N,p) \leq \frac{N}{2}) \;\leq\; \exp\Big(-2N\,(p - \frac{1}{2})^2\Big). \quad (14)$$

Summary of the theoretical findings. If $p > q$, Proposition 1 shows exponential decay of the error in N; if $q > p$, majority vote amplifies the wrong label. Hence: (1) self-consistent TTS improves with larger N *in regimes where the true class has the largest single-pass probability*, and (2) it is *effective only when the LLM is sufficiently confident*, in the sense of a nontrivial margin $p > q$.

Under the symmetry condition (Proposition 2), which is the best case, the lower bound of success can be analytically obtained, for any p. In the worst case (Proposition 3), similarly, the success rate can be analytically obtained.

3. Results and Discussion

3.1. Datasets and Models

To provide an initial proof of concept for our framework, we first evaluate it on text-based medical QA tasks using the Massive Multitask Language Understanding (MMLU) benchmark [7]. We focus on six medically relevant domains: clinical knowledge, medical genetics, anatomy, professional medicine, college biology, and college medicine. Since these are multiple-choice questions, all answer options are included in the prompt along with the question.

To further assess generalizability across modalities and disease types in VQA tasks, we conduct three disease classification tasks using PneumoniaMNIST, PathMNIST, and RetinaMNIST from MedMNIST v2 [36]. Specifically, pneumonia detection is performed using PneumoniaMNIST, which consists of 390 pneumonia cases and 234 normal cases from frontal X-ray images. PathMNIST is utilized for colorectal cancer classification, containing 1,233 cases of colorectal adenocarcinoma epithelium and 741 cases of normal colon mucosa. Diabetic retinopathy (DR) classification is explored with RetinaMNIST, which includes 226 cases of referable (i.e., non-proliferative or proliferative DR) and 174 normal cases from fundus images. All images are standardized to a resolution of 224 × 224 pixels.

For the MMLU benchmark, we primarily evaluate LLAMA-3.1-8B-INSTRUCT [28] and DEEPSEEK-R1-DISTILL-LLAMA-8B [5], as as well as additional results with LLAMA-3.2-1B-INSTRUCT and LLAMA-3.2-3B-INSTRUCT. For the VQA tasks, we employ LLAMA-3.2-11B-VISION-INSTRUCT [28]. Since the second stage of our two-stage inference framework admits flexible model selection, we further experiment with smaller text-only Llama models (1B, 3B, and 8B) as well as the medical-domain–specific MED42-V2-8B model [3].

The detailed prompts for each task and inference setting are provided in the Appendix C.

3.2. Comparison with Baselines

We begin by comparing the proposed framework against conventional baselines. For each dataset, we evaluate three test-time inference settings: (1) direct answering, (2) one-stage CoT, and (3) the proposed two-stage reasoning framework for VQA tasks. Then, each setting is further assessed both with and without the proposed TTS strategy.

Table 1 and Table 2 show that the proposed TTS strategy consistently delivers substantial performance gains across diverse tasks, models, and test-time inference strategies. While one-stage CoT without TTS often yields marginal or negative gains, TTS shows strong effects on vision-centric tasks through multi-sample aggregation. Our analysis further reveals several key observations:

- **Consistent gains across tasks and models.** On the MMLU dataset (Table 1), our TTS yields steady improvements across all six medical knowledge areas, up to 17.5 percentage points (pp). Similarly, for MedMNIST tasks (Table 2), TTS consistently boosts AUC and AP scores across image modalities, with gains up to 30.4 pp. These results indicate that the advantage of TTS is not task- or model-specific, but generalizes across text-based and vision-based medical tasks.
- **TTS outperforms CoT.** While prompt engineering alone often yields marginal or unstable effects, as reflected in the performance gap between direct answering and one-stage CoT, applying TTS consistently produces gains regardless of the initial prompting strategy. This highlights that TTS acts as a more reliable mechanism for enhancing model performance than simply reformatting instructions.
- **Strong effects on vision tasks.** Our TTS strategy achieves its most pronounced improvements on vision-centric tasks (Table 2). A single-pass VLM often overlooks subtle visual cues or produces ambiguous descriptions, whereas the multi-sample nature of TTS allows diverse perspectives to be aggregated into a more reliable representation. By generating multiple complementary descriptions, TTS filters out irrelevant features and converges on disease-relevant reasoning, thereby improving reliability. Importantly, these substantial improvements arise not from prompt design alone but from the synergy between structured reasoning and TTS, with scaling serving as the key driver of robustness in complex vision tasks.

3.3. Scaling Laws for Test-Time Compute

We analyze the effectiveness of TTS for medical image diagnosis in detail. As illustrated in Figure 2, we systematically vary the number of TTS samples, ranging from $N = 1$ (i.e., single-pass inference) up to $N = 64$ for text-based MMLU benchmarks and up to $N = 16$ for vision-based

Method	Clinical Knowledge	Medical Genetics	Anatomy	Professional Medicine	College Biology	College Medicine
Llama-3.1-8B-Instruct						
Direct Answering	0.71	0.75	0.62	0.73	0.75	0.64
Direct Answering (**+TTS**)	0.72 (↑ 1.3pp)	0.78 (↑ 3.5pp)	0.65 (↑ 2.8pp)	0.77 (↑ 3.6pp)	0.77 (↑ 2.3pp)	0.67 (↑ 3.1pp)
One-stage CoT	0.71	0.77	0.66	0.71	0.73	0.65
One-stage CoT (**+TTS**)	**0.80 (↑ 9.2pp)**	**0.84 (↑ 7.6pp)**	**0.72 (↑ 5.7pp)**	**0.85 (↑ 14.3pp)**	**0.84 (↑ 11.2pp)**	**0.77 (↑ 11.8pp)**
DeepSeek-R1-Distill-Llama-8B						
Direct Answering	0.52	0.55	0.48	0.46	0.54	0.47
Direct Answering (**+TTS**)	0.56 (↑ 3.8pp)	0.62 (↑ 6.8pp)	0.51 (↑ 3.4pp)	0.57 (↑ 10.6pp)	0.62 (↑ 8.1pp)	0.52 (↑ 5.0pp)
One-stage CoT	0.61	0.63	0.53	0.58	0.65	0.58
One-stage CoT (**+TTS**)	**0.73 (↑ 12.1pp)**	**0.80 (↑ 17.5pp)**	**0.64 (↑ 11.3pp)**	**0.72 (↑ 14.4pp)**	**0.80 (↑ 15.2pp)**	**0.74 (↑ 15.5pp)**

Table 1. Accuracy on six medical domains of MMLU using different prompting strategies. We compare **baselines** (direct answering and one-stage chain-of-thought (CoT)) with our **test-time scaling (TTS)** variants for $N = 64$. Across both LLAMA-3.1-8B-INSTRUCT and DEEPSEEK-R1-DISTILL-LLAMA-8B, applying TTS consistently improves performance over their respective baselines, with the largest gains observed for one-stage CoT, up to 17.5 percentage points (pp).

Method	Pneumonia		Colorectal Cancer		Diabetic Retinopathy	
	AUC	AP	AUC	AP	AUC	AP
Llama-3.2-11B-Vision-Instruct						
Direct Answering	0.50	0.62	0.56	0.65	0.61	0.63
Direct Answering (**+TTS**)	0.74 (↑ +24.2pp)	0.79 (↑ +16.9pp)	0.56 (↑ +0.5pp)	0.66 (↑ +0.3pp)	**0.71 (↑ +10.0pp)**	0.74 (↑ +11.1pp)
One-stage CoT	0.53	0.64	0.48	0.62	0.58	0.61
One-stage CoT (**+TTS**)	0.78 (↑ +24.9pp)	0.83 (↑ +18.8pp)	0.53 (↑ +5.4pp)	0.64 (↑ +2.4pp)	0.67 (↑ +9.2pp)	**0.74 (↑ +13.4pp)**
Two-stage Reasoning	0.52	0.63	0.54	0.65	0.57	0.61
Two-stage Reasoning (**+TTS**)	**0.82 (↑ +30.4pp)**	**0.86 (↑ +22.8pp)**	**0.65 (↑ +10.9pp)**	**0.75 (↑ +10.6pp)**	**0.71 (↑ +13.5pp)**	**0.74 (↑ +13.0pp)**

Table 2. Results on three MedMNIST datasets: PneumoniaMNIST (pneumonia detection), PathMNIST (colorectal cancer classification), and RetinaMNIST (diabetic retinopathy detection). We compare **baselines** (direct answering, one-stage CoT, and two-stage reasoning) with their **test-time scaling (TTS)** variants for $N = 16$. Across all datasets, applying TTS yields substantial and consistent improvements, with the two-stage reasoning + TTS method achieving the best overall performance. Largest gains observed for two-stage reasoning, up to 30.4 percentage points (pp). Metrics reported are AUC (area under the ROC curve) and AP (area under the precision–recall curve).

disease classification tasks, and evaluate the resulting model performance.

Figure 2 presents that **performance follows a power-law trend**, particularly up to medium sample sizes (e.g., $N \leq 16$): accuracy improve substantially as the number of samples increases. By aggregating across multiple complementary reasoning processes, the model reduces its reliance on any single, potentially flawed explanation. More comprehensive results are reported in Figure 4 in the Appendix.

This scaling behavior parallels our theoretical findings in Corollary 1 in Section 2.3 as well as prior observations in Beeching et al. [2] in language model reasoning tasks, where increasing test-time compute improves accuracy in a predictable manner. Importantly, the observed gains in medical image diagnosis suggest that such scaling laws extend beyond mathematical reasoning to (multimodal) medical applications.

From a practical standpoint, this result underscores a critical lesson: **relying on a single model output is unreliable in medical tasks**, as LLMs can generate plausible yet misleading information in specialized contexts[1]. In con-

[1]For instance, across all test-time inference methods, single-sample inference occasionally yields AUCs of only 50–60% on disease classification tasks.

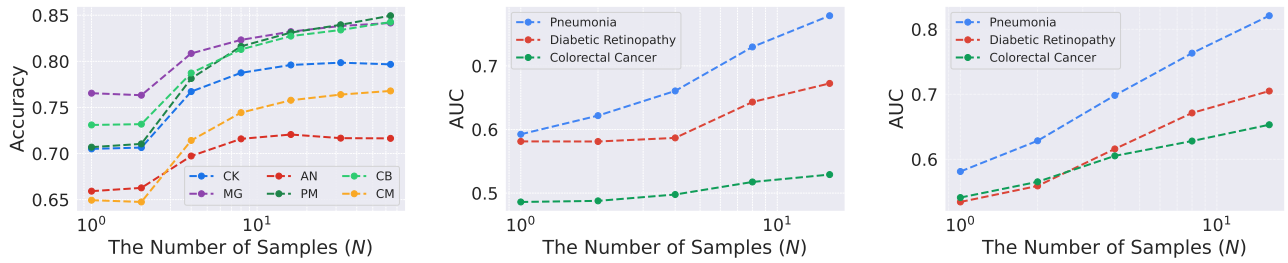

(a) One-stage CoT (Text) (b) One-stage CoT (Vision) (c) Two-Stage Reasoning (Vision)

Figure 2. A study examining the effect of sample size (N) in TTS setting. Increasing the sample size boosts performance across different datasets and inference methods, following a power law. LLAMA-3.1-8B-INSTRUCT and LLAMA-3.2-11B-VISION-INSTRUCT are used for text and vision tasks, respectively.

trast, test-time compute elevates diagnostic performance up to about 80% without requiring additional fine-tuning or retraining This highlights TTS as a promising avenue for improving both reliability and safety in real-world medical AI deployment.

3.4. Ablation on LLM Size in the Second Stage

We further note that the two-stage reasoning framework not only demonstrates empirical superiority but also provides practical advantages. By explicitly separates the extraction of raw visual information from the reasoning about clinical decisions, enabling flexible combinations of models across stages. In this setup, VLMs are generally more specialized in capturing and describing visual features, whereas LLMs are better suited for following instructions and providing structured reasoning. This separation allows practitioners to select a VLM best suited for image analysis while pairing it with an LLM tailored to the target clinical domain. To evaluate this flexibility, we replace the original Llama model in Stage 2 with a medical domain-specific model, MED42-V2-8B; we observe that it achieves slightly better performance (Figure 3).

More importantly, the modularity of this design opens the door to adaptive scaling. Since smaller LLMs (e.g., 3B parameters) can still provide sufficient reasoning capability, they can be employed in the second stage instead of the larger VLM used in the first stage (e.g., 11B), thereby reducing relative inference cost. To evaluate this property, we replace the original 11B LLM in Stage 2 with smaller models of 1B, 3B, and 8B parameters. As shown in Figure 3, performance remains high even with a 3B model, closely matching that of its 8B and 11B counterparts. Notably, for pneumonia diagnosis, even a 1B model achieves reasonable performance.

3.5. Model Capacity Matters for TTS

So far, we have observed that TTS consistently improves the zero-shot performance of reasoning models and exhibits

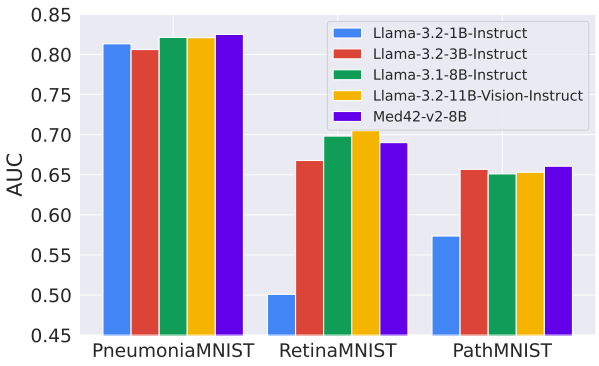

Figure 3. The proposed method's flexibility by replacing the Stage 2 LLM with models of varying sizes. A 3B model performs comparably to an 11B model, demonstrating the benefit of using the two-stage framework.

stronger synergy with models that already possess sufficient reasoning ability (e.g., models of size 8B and above). To further investigate this trend, we conduct an ablation study on the MMLU dataset using substantially smaller reasoning models.

As reported in Table 3, smaller 1B and 3B models demonstrate limited reasoning capability in medical QA tasks. Nonetheless, TTS provides a modest boost with smaller models when direct answering is applied. However, applying a standard one-stage CoT prompt substantially degrades the performance of smaller models. For instance, with LLAMA-3.2-1B-INSTRUCT, accuracy drops from 0.346 to 0.160 in Clinical Knowledge, effectively cutting performance by more than half across all domains. Moreover, introducing TTS on top of one-stage CoT further amplifies this degradation, driving accuracy down to 0.039 in Clinical Knowledge.

These results highlight the effectiveness of TTS depends critically on the baseline competence of the underlying

Method	Clinical Knowledge	Medical Genetics	Anatomy	Professional Medicine	College Biology	College Medicine
Llama-3.2-1B-Instruct						
Direct Answering	0.35	0.34	0.41	0.31	0.35	0.33
Direct Answering (**+TTS**)	**0.41** (↑ 6.2pp)	**0.39** (↑ 4.7pp)	**0.47** (↑ 6.5pp)	**0.38** (↑ 6.1pp)	**0.40** (↑ 4.4pp)	**0.39** (↑ 5.8pp)
One-stage CoT	0.16	0.16	0.21	0.15	0.18	0.17
One-stage CoT (**+TTS**)	0.04 (↓ 12.1pp)	0.02 (↓ 14.1pp)	0.08 (↓ 12.8pp)	0.01 (↓ 13.9pp)	0.05 (↓ 12.5pp)	0.07 (↓ 9.6pp)
Llama-3.2-3B-Instruct						
Direct Answering	0.60	0.65	0.57	0.68	0.65	0.54
Direct Answering (**+TTS**)	**0.64** (↑ 3.7pp)	**0.70** (↑ 4.4pp)	**0.64** (↑ 6.6pp)	**0.77** (↑ 8.7pp)	**0.70** (↑ 5.1pp)	**0.55** (↑ 0.8pp)
One-stage CoT	0.45	0.49	0.48	0.39	0.38	0.38
One-stage CoT (**+TTS**)	0.57 (↑ 12.4pp)	0.66 (↑ 17.1pp)	0.62 (↑ 14.5pp)	0.50 (↑ 11.2pp)	0.45 (↑ 7.8pp)	0.45 (↑ 7.2pp)

Table 3. Accuracy on six medical domains of MMLU using different prompting strategies. We compare **baselines** (direct answering and one-stage chain-of-thought (CoT)) with their **test-time scaling (TTS)** variants using $N = 64$. For LLAMA-3.2-1B-INSTRUCT, CoT prompting substantially degrades performance, and applying TTS further amplifies this degradation. In contrast, for LLAMA-3.2-3B-INSTRUCT, CoT also lowers baseline accuracy, but TTS recovers and yields consistent improvements across all domains. Overall, these results suggest that TTS is most effective when the underlying model achieves at least non-trivial accuracy (above random guessing, i.e., $\sim$25% for four-choice questions); otherwise, scaling may reinforce biased or uninformative reasoning.

models, and that naively introducing reasoning prompts can be counterproductive—as we show in Proposition 1 in Section 2.3. When the model exhibits at least non-trivial zero-shot accuracy, TTS can enhance and stabilize reasoning. Conversely, when the model struggles to reason in the first place, scaling may only reinforce biased or uninformative outputs, limiting its practical utility.

4. Conclusion

In this work, we propose a fine-tuning–free framework for medical tasks, including medical image diagnosis, that leverages test-time scaling (TTS) to enhance clinical reasoning. By systematically analyzing both text- and vision-based medical benchmarks, we demonstrate that TTS consistently improves performance over single-pass baselines, with gains of up to 30.4 percentage points. Our theoretical analysis further provide scaling laws that explain how and when such improvements emerge, establishing a foundation for principled use of TTS in medicine.

The first central question guiding this study is: *under what conditions does TTS improve performance?* Our findings indicate that TTS is most beneficial when the underlying model possesses at least non-trivial baseline competence, as scaling amplifies informative reasoning while suppressing noise. Conversely, when baseline reasoning is weak, scaling alone cannot guarantee reliable improvements. Another key question is: *can these methods extend beyond text to multimodal medical VQA tasks?* Our experiments confirm that TTS generalizes beyond text, yielding strong effects on vision-centric tasks by aggregating multiple complementary descriptions into relevant reasoning.

Implications and Future Directions. Even with significant gains in AI for medicine, concerns persist due to the inherent "black-box" nature of conventional deep learning models. In contrast, LLMs generate intermediate reasoning, offering transparency that helps mitigate black-box concerns, while enhancing performance in clinical applications. However, the scarcity of high-quality medical annotations required to train verifiers or process reward models makes such approaches difficult to apply in practice. To address this, our work focuses on a simple yet effective parallel thinking–based TTS method, providing a foundational demonstration of how zero-shot performance can be improved without costly supervision. In the future, more sophisticated reward-model-based strategies may become feasible as domain-specific resources expand.

Looking forward, our framework opens several avenues for future work. One promising direction is to explore adaptive TTS strategies that dynamically allocate compute based on task difficulty or model uncertainty, further improving efficiency in clinical settings. Another is to investigate how TTS interacts with domain-specialized models or multimodal foundation models, potentially enabling broader deployment. Finally, rigorous human-in-the-loop studies will be essential to assess how TTS-enhanced reasoning integrates with real-world clinical workflows, ensuring that these methods support trustworthy decision-making and ultimately improve patient outcomes.

References

[1] Emmanuel Abbe, Samy Bengio, Aryo Lotfi, Colin Sandon, and Omid Saremi. How far can transformers reason? the globality barrier and inductive scratchpad. *Advances in Neural Information Processing Systems*, 37:27850–27895, 2025. 2

[2] Edward Beeching, Lewis Tunstall, and Sasha Rush. Scaling test-time compute with open models. 4, 6

[3] Clément Christophe, Praveen K Kanithi, Tathagata Raha, Shadab Khan, and Marco AF Pimentel. Med42-v2: A suite of clinical llms. *arXiv preprint arXiv:2408.06142*, 2024. 5

[4] Karl Cobbe, Vineet Kosaraju, Mohammad Bavarian, Mark Chen, Heewoo Jun, Lukasz Kaiser, Matthias Plappert, Jerry Tworek, Jacob Hilton, Reiichiro Nakano, et al. Training verifiers to solve math word problems. *arXiv preprint arXiv:2110.14168*, 2021. 2, 11

[5] DeepSeek-AI. Deepseek-r1: Incentivizing reasoning capability in llms via reinforcement learning, 2025. 5

[6] Chuan Guo, Geoff Pleiss, Yu Sun, and Kilian Q Weinberger. On calibration of modern neural networks. In *International conference on machine learning*, pages 1321–1330. PMLR, 2017. 3

[7] Dan Hendrycks, Collin Burns, Steven Basart, Andy Zou, Mantas Mazeika, Dawn Song, and Jacob Steinhardt. Measuring massive multitask language understanding. *arXiv preprint arXiv:2009.03300*, 2020. 5

[8] Dan Hendrycks, Collin Burns, Saurav Kadavath, Akul Arora, Steven Basart, Eric Tang, Dawn Song, and Jacob Steinhardt. Measuring mathematical problem solving with the math dataset. *arXiv preprint arXiv:2103.03874*, 2021. 11

[9] Xiaoke Huang, Juncheng Wu, Hui Liu, Xianfeng Tang, and Yuyin Zhou. m1: Unleash the potential of test-time scaling for medical reasoning with large language models. *arXiv preprint arXiv:2504.00869*, 2025. 11

[10] Douglas Johnson, Rachel Goodman, J Patrinely, Cosby Stone, Eli Zimmerman, Rebecca Donald, Sam Chang, Sean Berkowitz, Avni Finn, Eiman Jahangir, et al. Assessing the accuracy and reliability of ai-generated medical responses: an evaluation of the chat-gpt model. *Research square*, pages rs–3, 2023. 1, 11

[11] Takeshi Kojima, Shixiang Shane Gu, Machel Reid, Yutaka Matsuo, and Yusuke Iwasawa. Large language models are zero-shot reasoners. *Advances in neural information processing systems*, 35:22199–22213, 2022. 2

[12] Jason J Lau, Soumya Gayen, Asma Ben Abacha, and Dina Demner-Fushman. A dataset of clinically generated visual questions and answers about radiology images. *Scientific data*, 5(1):1–10, 2018. 11

[13] Chunyuan Li, Cliff Wong, Sheng Zhang, Naoto Usuyama, Haotian Liu, Jianwei Yang, Tristan Naumann, Hoifung Poon, and Jianfeng Gao. Llava-med: Training a large language-and-vision assistant for biomedicine in one day. *Advances in Neural Information Processing Systems*, 36:28541–28564, 2023. 1, 11

[14] Chengshu Li, Ruohan Zhang, Josiah Wong, Cem Gokmen, Sanjana Srivastava, Roberto Martín-Martín, Chen Wang, Gabrael Levine, Michael Lingelbach, Jiankai Sun, et al. Behavior-1k: A benchmark for embodied ai with 1,000 everyday activities and realistic simulation. In *Conference on Robot Learning*, pages 80–93. PMLR, 2023. 1, 11

[15] Hunter Lightman, Vineet Kosaraju, Yuri Burda, Harrison Edwards, Bowen Baker, Teddy Lee, Jan Leike, John Schulman, Ilya Sutskever, and Karl Cobbe. Let's verify step by step. In *The Twelfth International Conference on Learning Representations*, 2024. 2

[16] Jiaxiang Liu, Yuan Wang, Jiawei Du, Joey Tianyi Zhou, and Zuozhu Liu. Medcot: Medical chain of thought via hierarchical expert. *arXiv preprint arXiv:2412.13736*, 2024. 1, 11

[17] Aman Madaan, Niket Tandon, Prakhar Gupta, Skyler Hallinan, Luyu Gao, Sarah Wiegreffe, Uri Alon, Nouha Dziri, Shrimai Prabhumoye, Yiming Yang, et al. Self-refine: Iterative refinement with self-feedback. *Advances in Neural Information Processing Systems*, 36:46534–46594, 2023. 11

[18] Michael Moor, Qian Huang, Shirley Wu, Michihiro Yasunaga, Yash Dalmia, Jure Leskovec, Cyril Zakka, Eduardo Pontes Reis, and Pranav Rajpurkar. Med-flamingo: a multimodal medical few-shot learner. In *Machine Learning for Health (ML4H)*, pages 353–367. PMLR, 2023. 1, 11

[19] Vishwesh Nath, Wenqi Li, Dong Yang, Andriy Myronenko, Mingxin Zheng, Yao Lu, Zhijian Liu, Hongxu Yin, Yee Man Law, Yucheng Tang, et al. Vila-m3: Enhancing vision-language models with medical expert knowledge. In *Proceedings of the Computer Vision and Pattern Recognition Conference*, pages 14788–14798, 2025. 11

[20] Tianwen Qian, Jingjing Chen, Linhai Zhuo, Yang Jiao, and Yu-Gang Jiang. Nuscenes-qa: A multi-modal visual question answering benchmark for autonomous driving scenario. In *Proceedings of the AAAI Conference on Artificial Intelligence*, pages 4542–4550, 2024. 1, 11

[21] Yuxiao Qu, Tianjun Zhang, Naman Garg, and Aviral Kumar. Recursive introspection: Teaching language model agents how to self-improve. *Advances in Neural Information Processing Systems*, 37:55249–55285, 2024. 11

[22] Jonathan Roberts, Kai Han, Neil Houlsby, and Samuel Albanie. Scifibench: Benchmarking large multimodal models for scientific figure interpretation. *Advances in Neural Information Processing Systems*, 37:18695–18728, 2024. 1, 11

[23] Karan Singhal, Shekoofeh Azizi, Tao Tu, S Sara Mahdavi, Jason Wei, Hyung Won Chung, Nathan Scales, Ajay Tanwani, Heather Cole-Lewis, Stephen Pfohl, et al. Large language models encode clinical knowledge. *Nature*, 620 (7972):172–180, 2023. 4

[24] Karan Singhal, Tao Tu, Juraj Gottweis, Rory Sayres, Ellery Wulczyn, Mohamed Amin, Le Hou, Kevin Clark, Stephen R Pfohl, Heather Cole-Lewis, et al. Toward expert-level medical question answering with large language models. *Nature Medicine*, 31(3):943–950, 2025. 2, 4

[25] Charlie Snell, Jaehoon Lee, Kelvin Xu, and Aviral Kumar. Scaling llm test-time compute optimally can be more effective than scaling model parameters. *arXiv preprint arXiv:2408.03314*, 2024. 1, 2, 3, 11

[26] Aarohi Srivastava, Abhinav Rastogi, Abhishek Rao, Abu Awal Shoeb, Abubakar Abid, Adam Fisch, Adam R

Brown, Adam Santoro, Aditya Gupta, Adri Garriga-Alonso, et al. Beyond the imitation game: Quantifying and extrapolating the capabilities of language models. *Transactions on machine learning research*, 2023. 11

[27] Mohamad-Hani Temsah, Amr Jamal, Khalid Alhasan, Abdulkarim A Temsah, and Khalid H Malki. Openai o1-preview vs. chatgpt in healthcare: a new frontier in medical ai reasoning. *Cureus*, 16(10), 2024. 1, 11

[28] Hugo Touvron, Thibaut Lavril, Gautier Izacard, Xavier Martinet, Marie-Anne Lachaux, Timothée Lacroix, Baptiste Rozière, Naman Goyal, Eric Hambro, Faisal Azhar, et al. Llama: Open and efficient foundation language models. *arXiv preprint arXiv:2302.13971*, 2023. 5

[29] Tao Tu, Shekoofeh Azizi, Danny Driess, Mike Schaekermann, Mohamed Amin, Pi-Chuan Chang, Andrew Carroll, Charles Lau, Ryutaro Tanno, Ira Ktena, et al. Towards generalist biomedical ai. *Nejm Ai*, 1(3):AIoa2300138, 2024. 1, 11

[30] Tao Tu, Mike Schaekermann, Anil Palepu, Khaled Saab, Jan Freyberg, Ryutaro Tanno, Amy Wang, Brenna Li, Mohamed Amin, Yong Cheng, et al. Towards conversational diagnostic artificial intelligence. *Nature*, pages 1–9, 2025. 1, 11

[31] Jonathan Uesato, Nate Kushman, Ramana Kumar, Francis Song, Noah Siegel, Lisa Wang, Antonia Creswell, Geoffrey Irving, and Irina Higgins. Solving math word problems with process-and outcome-based feedback. *arXiv preprint arXiv:2211.14275*, 2022. 2, 11

[32] Peiyi Wang, Lei Li, Zhihong Shao, R. X. Xu, Damai Dai, Yifei Li, Deli Chen, Y. Wu, and Zhifang Sui. Math-shepherd: Verify and reinforce llms step-by-step without human annotations. *CoRR*, abs/2312.08935, 2023. 2, 11

[33] Xuezhi Wang, Jason Wei, Dale Schuurmans, Quoc Le, Ed Chi, Sharan Narang, Aakanksha Chowdhery, and Denny Zhou. Self-consistency improves chain of thought reasoning in language models. *arXiv preprint arXiv:2203.11171*, 2022. 2, 3, 11

[34] Jason Wei, Xuezhi Wang, Dale Schuurmans, Maarten Bosma, Fei Xia, Ed Chi, Quoc V Le, Denny Zhou, et al. Chain-of-thought prompting elicits reasoning in large language models. *Advances in neural information processing systems*, 35:24824–24837, 2022. 1, 11

[35] Zhengzhuo Xu, Sinan Du, Yiyan Qi, Chengjin Xu, Chun Yuan, and Jian Guo. Chartbench: A benchmark for complex visual reasoning in charts. *arXiv preprint arXiv:2312.15915*, 2023. 1, 11

[36] Jiancheng Yang, Rui Shi, Donglai Wei, Zequan Liu, Lin Zhao, Bilian Ke, Hanspeter Pfister, and Bingbing Ni. Medmnist v2-a large-scale lightweight benchmark for 2d and 3d biomedical image classification. *Scientific Data*, 10(1):41, 2023. 5

[37] Wenkai Yang, Shuming Ma, Yankai Lin, and Furu Wei. Towards thinking-optimal scaling of test-time compute for llm reasoning. *arXiv preprint arXiv:2502.18080*, 2025. 11

[38] Shunyu Yao, Dian Yu, Jeffrey Zhao, Izhak Shafran, Tom Griffiths, Yuan Cao, and Karthik Narasimhan. Tree of thoughts: Deliberate problem solving with large language models. *Advances in neural information processing systems*, 36:11809–11822, 2023. 2, 3, 11

[39] Zhenru Zhang, Chujie Zheng, Yangzhen Wu, Beichen Zhang, Runji Lin, Bowen Yu, Dayiheng Liu, Jingren Zhou, and Junyang Lin. The lessons of developing process reward models in mathematical reasoning. *arXiv preprint arXiv:2501.07301*, 2025. 2

[40] Yuxin Zuo, Shang Qu, Yifei Li, Zhangren Chen, Xuekai Zhu, Ermo Hua, Kaiyan Zhang, Ning Ding, and Bowen Zhou. Medxpertqa: Benchmarking expert-level medical reasoning and understanding. *arXiv preprint arXiv:2501.18362*, 2025. 11

A. Related Work

A.1. Vision-Language Models in Medical Imaging

Conventional data-driven deep learning approaches parameterize a model with learnable parameters and train it on a dataset of image–label pairs. Such models are often treated as *black-box* predictors: they provide a final classification result but lack transparency, the reasoning underlying the diagnostic process non-interpretable. Given the safety-critical nature of medicine and the risk that generated content may deviate from clinical standards, rigorous evaluation is mandated to assess progress and mitigate harms [10]. Addressing these interpretability and reliability concerns is paramount for the responsible deployment of AI in clinical settings.

On the other hand, the development of VLMs has rapidly progressed, enabling models to process both images and text for diverse applications, including robotics [14], autonomous driving [20], and scientific research [22, 35]. In the medical domain, early efforts focused on foundational tasks such as medical image captioning and VQA on datasets like VQA-RAD [12]. More recently, models like Med-PaLM [29], Med-Flamingo [18], and LLaVA-Med [13] have demonstrated strong performance in generating clinically-relevant text. These efforts are now being pushed further by more recent works such as VILA-M3 [19] and MedXpertQA [40], which focus on more complex reasoning and comprehensive evaluations.

The use of multi-stage reasoning, a paradigm that breaks down a complex task into a series of intermediate steps, has gained significant traction as an alternative to end-to-end approaches. This aligns with the clinical workflow, where a clinician first observes an image and other patient information, analyzes the symptoms, and then formulates a diagnosis based on their observations and knowledge. For instance, recent works have explicitly incorporated multi-stage reasoning, such as CoT [16, 30], to generate detailed diagnostic rationales and explain their decision-making process. More advanced methods have also emerged, including Tree-of-Thought (ToT) [38], which creates a tree-like structure of potential diagnostic paths and evidence. This allows the model to explore and evaluate multiple hypotheses simultaneously before reaching a final conclusion.

A.2. Test-Time Compute Scaling

TTS has become a prominent research area, offering a computationally efficient alternative to traditional retraining for enhancing model performance. By leveraging an increased computational budget at inference time, these strategies improve a model's accuracy and robustness without requiring any changes to its parameters or architecture. CoT [27, 34] is a notable example, where a model is prompted to generate a series of intermediate reasoning steps before arriving at the final answer. While effective, CoT can be sensitive to prompting and may not always yield consistent results. TTS, a related but distinct paradigm, further improves performance by moving beyond a single, deterministic output. Instead, TTS methods sample multiple candidate outputs and aggregate them to form a more robust and reliable final prediction.

A variety of TTS strategies have been explored, ranging from simple aggregation to more complex reasoning-based methods. Simple approaches like self-consistency [33] and majority voting rely on aggregating multiple generated outputs to improve reliability. More advanced techniques have significantly pushed performance boundaries on complex benchmarks. For instance, self-refinement [17, 21] is an iterative approach where a model critiques its own output and then revises it in a feedback loop. Similarly, verifier-based methods [4, 31] and process reward models [32] have achieved state-of-the-art results by training a separate model to select the best output. Recent works have validated these approaches on increasingly challenging benchmarks, such as MATH [8], GSM8K [4], and the BIG-Bench Hard suite [26], demonstrating their strong performance in mathematical and symbolic reasoning tasks.

Although powerful AI techniques are promising, their application in medicine is still emerging. One direction for improving model performance is scaling "*deep thinking*" by increasing a model's computational budget for a single reasoning path, such as by expanding its token limit [9]. However, this approach faces significant challenges: it can lead to overthinking [37]. Consequently, "*parallel thinking*" strategies represent another important yet unexplored avenue in the medical domain. A key barrier to those advanced methods (e.g., Best-of-N, and beam search [25]) is their reliance on reward models, which are often unavailable in medicine as they demand vast amounts of labeled data for training [2]. To this end, this paper explores the application of a reward-free TTS to medical image diagnosis by extending a majority voting strategy into a probabilistic framework that not only improves reliability.

B. Omitted Proofs

Proof of Lemma 1.

Proof. For the first case, we bound the probability of error by applying a union bound over all possible failure modes. An error occurs if at least one competitor class $j \neq c^\star$ re-

[2] This data is not merely correct answers but expert-annotated process supervision, where a model's step-by-step reasoning is evaluated. The high cost of clinical experts' time and the inherent complexity of medical judgment make acquiring this type of data prohibitively expensive and scarce.

ceives at least as many votes as the true class $c^\star$.

$$\begin{aligned}\mathbb{P}(\hat{y}_{\mathrm{MV}} \neq c^\star) &= \mathbb{P}\Big(\bigcup_{j\neq c^\star}\{X_j \geq X_{c^\star}\}\Big) \\ &\leq \sum_{j\neq c^\star}\mathbb{P}(X_j \geq X_{c^\star}).\end{aligned} \tag{15}$$

For each competitor j, let $D_j := X_{c^\star} - X_j$. The term $\mathbb{P}(X_j \geq X_{c^\star})$ is equivalent to $\mathbb{P}(D_j \leq 0)$. The quantity D_j is a sum of N i.i.d. random variables $V_i = \mathbf{1}\{y_i = c^\star\} - \mathbf{1}\{y_i = j\}$, where each $V_i \in \{-1, 0, 1\}$. The expectation is $\mathbb{E}[D_j] = N(p - p_j)$. By Hoeffding's inequality (with variable range $1 - (-1) = 2$):

$$\begin{aligned}\mathbb{P}(D_j \leq 0) &= \mathbb{P}(D_j - \mathbb{E}[D_j] \leq -N(p - p_j)) \\ &\leq \exp\Big(-\frac{2(N(p-p_j))^2}{N\cdot 2^2}\Big) \\ &= \exp\Big(-\frac{N}{2}(p-p_j)^2\Big).\end{aligned} \tag{16}$$

Since $q = \max_{k\neq c^\star} p_k$, we have $p - p_j \geq p - q$ for all $j \neq c^\star$. This implies $(p-p_j)^2 \geq (p-q)^2$. We can thus bound each term in the sum by the worst case:

$$\begin{aligned}\mathbb{P}(\hat{y}_{\mathrm{MV}} \neq c^\star) &\leq \sum_{j\neq c^\star}\exp\Big(-\frac{N}{2}(p-p_j)^2\Big) \\ &\leq \sum_{j\neq c^\star}\exp\Big(-\frac{N}{2}(p-q)^2\Big) \\ &= (C-1)\,\exp\Big(-\frac{N}{2}(p-q)^2\Big).\end{aligned} \tag{17}$$

For the second case, let $j^\dagger \in \arg\max_{j\neq c^\star} p_j$ so that $p_{j^\dagger} = q$. For the true class $c^\star$ to win, it must receive more votes than any other class, including the strongest competitor $j^\dagger$. Thus, the event $\{\hat{y}_{\mathrm{MV}} = c^\star\}$ is a subset of the event $\{X_{c^\star} > X_{j^\dagger}\}$.

$$\mathbb{P}(\hat{y}_{\mathrm{MV}} = c^\star) \leq \mathbb{P}(X_{c^\star} > X_{j^\dagger}). \tag{18}$$

Let $D := X_{c^\star} - X_{j^\dagger}$. The expectation is $\mathbb{E}[D] = N(p - q) < 0$. We bound $\mathbb{P}(D > 0)$. By Hoeffding's inequality:

$$\begin{aligned}\mathbb{P}(D > 0) &= \mathbb{P}(D - \mathbb{E}[D] > -N(p-q)) \\ &= \mathbb{P}(D - \mathbb{E}[D] > N(q-p)) \\ &\leq \exp\Big(-\frac{N}{2}(q-p)^2\Big).\end{aligned} \tag{19}$$

□

Proof of Lemma 2.

Proof. Under symmetry, conditional on $X_{c^\star} = k$, the wrong counts are multinomial with equal cell probabilities, and each X_j is stochastically dominated by $\mathrm{Bin}(N, q_0)$. Thus

$$\begin{aligned}\mathbb{P}(\text{success}) &\geq \mathbb{P}(X_{c^\star} > t,\ \forall j \neq c^\star :\ X_j < t) \\ &\geq 1 - \mathbb{P}(X_{c^\star} \leq t) - \mathbb{P}(\exists j :\ X_j \geq t),\end{aligned} \tag{20}$$

and $\mathbb{P}(\exists j :\ X_j \geq t) \leq (C-1)\,\mathbb{P}(\mathrm{Bin}(N, q_0) \geq t)$.

The second inequality follows from a direct argument using the threshold $t = N/2$. The event $\{Y_{c^\star} > N/2\}$ is a subset of the event $\{\hat{y}_{\mathrm{MV}} = c^\star\}$, thus its probability provides a lower bound:

$$\mathbb{P}(\hat{y}_{\mathrm{MV}} = c^\star) \geq \mathbb{P}(Y_{c^\star} > N/2). \tag{21}$$

Given that $Y_{c^\star} \sim \mathrm{Bin}(N, p)$, we can express this probability as the sum over the binomial probability mass function for all successful outcomes. The smallest integer count k satisfying $k > N/2$ is $\lfloor N/2 \rfloor + 1$.

$$\begin{aligned}&\mathbb{P}(Y_{c^\star} > N/2) \\ &\quad= \sum_{k=\lfloor N/2\rfloor+1}^{N}\mathbb{P}(Y_{c^\star} = k) \\ &\quad= \sum_{k=\lfloor N/2\rfloor+1}^{N}\binom{N}{k}p^k(1-p)^{N-k}.\end{aligned} \tag{22}$$

Combining these results yields the final inequality, which completes the proof. □

Proof of Lemma 3.

Proof. With all wrong mass on a single class, the problem reduces to a binomial majority test between $c^\star$ and $j^\dagger$.

The probability of error is the event where the true class $c^\star$ is not the majority vote winner, $\mathbb{P}(\hat{y}_{\mathrm{MV}} \neq c^\star)$. For the purpose of establishing this upper bound, we use the conservative assumption that a tie is counted as a loss for the true class.

The error event is therefore $Y_{c^\star} \leq Y_{j^\dagger}$. We can express this condition entirely in terms of the true class count $Y_{c^\star}$:

$$\begin{aligned}Y_{c^\star} \leq Y_{j^\dagger} &\iff Y_{c^\star} \leq N - Y_{c^\star} \\ &\iff 2Y_{c^\star} \leq N \iff Y_{c^\star} \leq N/2.\end{aligned}$$

This directly establishes the first equality in the lemma:

$$\mathbb{P}(\hat{y}_{\mathrm{MV}} \neq c^\star) = \mathbb{P}(\mathrm{Bin}(N, p) \leq N/2). \tag{23}$$

To derive the final exponential bound, we apply Hoeffding's inequality. Let the N votes be a sequence of i.i.d. Bernoulli trials $V_1, \ldots, V_N$, where $V_i = 1$ if the vote is for $c^\star$ (with probability p) and $V_i = 0$ otherwise. The sample mean is $\bar{V} = Y_{c^\star}/N$, and its expectation is $\mathbb{E}[\bar{V}] = p$.

We rewrite the error probability in terms of the sample mean. The inequality follows by applying the one-sided

Hoeffding's inequality with a deviation of $\epsilon = p - 1/2$ below the mean (assuming $p > 1/2$).

$$\begin{aligned}\mathbb{P}(\hat{y}_{\mathrm{MV}} \neq c^\star) &= \mathbb{P}(\bar{V} \leq 1/2) \\ &= \mathbb{P}(\bar{V} - p \leq 1/2 - p) \\ &= \mathbb{P}(\bar{V} - p \leq -(p - 1/2)) \\ &\leq \exp\Big(- 2N\,(p - \frac{1}{2})^2 \Big).\end{aligned} \tag{24}$$

This is equivalent to the Lemma 1 with $q = 1 - p$ and $C = 2$. □

C. Prompts

For evaluation on the MMLU benchmark, we employed two primary prompt formats: direct answering and one-stage Chain-of-Thought (CoT). For medical image diagnosis on the MedMNIST dataset, we employed three prompt formats: direct answering, one-stage Chain-of-Thought (CoT), and our proposed two-stage reasoning.

C.1. Prompt Structure for MMLU Evaluation

C.1.1. Direct Answering Prompt

In the direct answering prompt, the model is instructed to select the correct letter choice without providing any intermediate explanation or reasoning. This setup evaluates the model's immediate knowledge of the subject matter. An example direct answering prompt is shown in the visualization below.

User Input

The following are multiple-choice questions (with answers) about {subject}. Provide your answer with "The answer is (X)" where X is the correct letter choice, with no additional explanation.

Question: {question}

Options: A. {o1}, B. {o2}, C. {o3}, D. {o4}

C.1.2. Chain-of-Thought (CoT) Prompt

The one-stage Chain-of-Thought (CoT) prompt instructs the model to produce step-by-step reasoning before selecting a final answer. We implement this by explicitly asking the model to "think step by step," then report the final letter choice. This setting assesses the model's reasoning ability in addition to its factual knowledge.

User Input

The following are multiple-choice questions (with answers) about {subject}. Think step by step and then finish your answer with "The answer is (X)" where X is the correct letter choice.

Question: {question}

Options: A. {o1}, B. {o2}, C. {o3}, D. {o4}

Assistant Response (Prefix)

Answer: Let's think step by step.

C.2. One-Stage Prompt Structure for MedMNIST

In medical imaging tasks with one-stage inference (i.e., direct answering and one-stage CoT), we use a direct-instruction format: the model receives a single-turn system prompt that specifies the classification task and the required output format. For one-stage CoT, we append the cue "Let's think step by step." to the prompt.

C.2.1. Pneumonia Detection

User Input

Your task is binary-class classification of 'pneumonia' against 'normal'. Given a given gray-scale pediatric chest X-Ray image, classify it as 0 (normal) or 1 (pneumonia). Make sure to put the answer (and only answer) inside `\boxed{}`.

C.2.2. Colorectal Cancer

User Input

Your task is binary-class classification of 'malignant: colorectal adenocarcinoma epithelium' against 'normal'. Given a hematoxylin & eosin stained histological image, classify it as 0 (normal) or 1 (malignant). Make sure to put the answer (and only answer) inside `\boxed{}`.

C.2.3. Diabetic Retinopathy

User Input

Your task is binary-class classification of 'diabetic retinopathy (DR)' against 'normal'. Given a retina fundus image, classify it as 0 (normal) or 1 (DR). Make sure to put the answer (and only answer) inside `\boxed{}`.

C.3. Two-Stage Prompt Structure for MedMNIST

In the two-stage reasoning setup for medical image diagnosis, the prompt is structured into two phases: (1) a general

instruction asking the model to summarize the visual features from a given image, and (2) a task-specific prompt that provides detailed guidelines and questions, combined with the summary generated in the first stage (referred to as the note).

C.3.1. Stage 1 Prompt for All Tasks

User Input

Summarize the list of key observable features detected in the image using bullet points.

C.3.2. Stage 2 Prompt for Pneumonia Detection

User Input

You are a healthcare professional to provide accurate pneumonia diagnosis.
Task:
- You will receive a report describing a patient's pediatric chest X-Ray image.
- Your goal is to classify:
- 0 = normal
- 1 = pneumonia

Guidelines:
1. Carefully read the note.
2. Decide which class (0 or 1) best matches the clinical features described. Assume that all of the relevant details have been explained in the text.
3. Provide your final answer enclosed in `\boxed{}` with no additional explanation, e.g., `\boxed{1}`.

IMPORTANT:
- Strictly adhere to the format by outputting only the final grade inside `\boxed{}` and nothing else.

Note:
{note}

—

Question:
Based on the above note, what is the correct pneumonia diagnosis? Please consider that all necessary details have been provided in the text above. Remember to provide only the class (0 or 1) inside `\boxed{}`.

C.3.3. Stage 2 Prompt for Colorectal Cancer

User Input

You are a pathologist to provide an accurate colorectal adenocarcinoma epithelium diagnosis.
Task:
- You will receive a report describing a patient's hematoxylin & eosin stained histological image.
- Your goal is to classify the tissue type:
- 0 = normal
- 1 = malignant (colorectal adenocarcinoma epithelium)

Guidelines:
1. Carefully read the note.
2. Decide which class (0 or 1) best matches the clinical features described. Assume that all of the relevant details have been explained in the text.
3. Provide your final answer enclosed in `\boxed{}` with no additional explanation, e.g., `\boxed{1}`.

IMPORTANT:
- Strictly adhere to the format by outputting only the final grade inside `\boxed{}` and nothing else.

Note:
{note}

—

Question:
Based on the above note, what is the correct tissue type? Please consider that all necessary details have been provided in the text above. Remember to provide only the class (0 or 1) inside `\boxed{}`.

C.3.4. Stage 2 Prompt for Diabetic Retinopathy

User Input

You are an ophthalmologist to provide accurate diabetic retinopathy (DR) diagnosis.
Task:
- You will receive a report describing a patient's retina fundus image.
- Your goal is to classify:
- 0 = normal
- 1 = referrable

Guidelines:
1. Carefully read the note.
2. Decide which class (0 or 1) best matches the clinical features described. Assume that all of the relevant details have been explained in the text.
3. Provide your final answer enclosed in `\boxed{}` with no additional explanation, e.g., `\boxed{1}`.

IMPORTANT:
- Strictly adhere to the format by outputting only the final grade inside `\boxed{}` and nothing else.

Note:
{note}

—

Question:
Based on the above note, what is the correct diabetic retinopathy (DR) diagnosis? Please consider that all necessary details have been provided in the text above. Remember to provide only the class (0 or 1) inside `\boxed{}`.

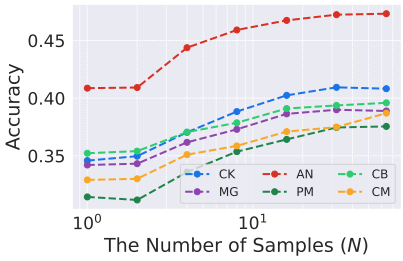

(a) Direct Answering (Text) w/ Llama-1B

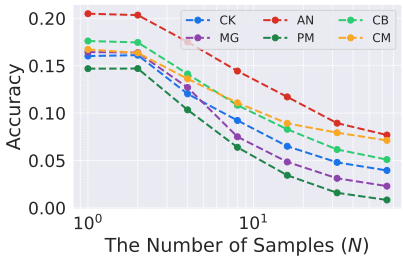

(b) One-stage CoT (Text) w/ Llama-1B

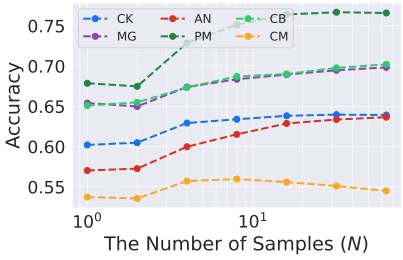

(c) Direct Answering (Text) w/ Llama-3B

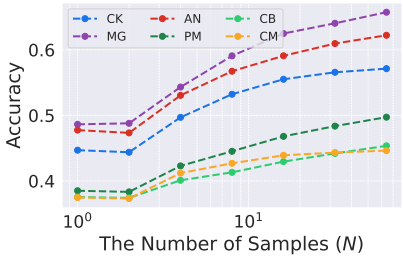

(d) One-stage CoT (Text) w/ Llama-3B

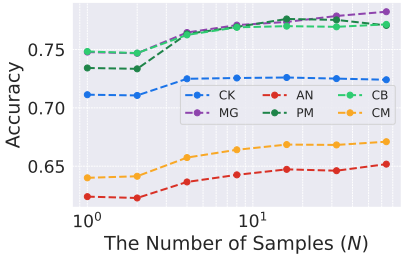

(e) Direct Answering (Text) w/ Llama-8B

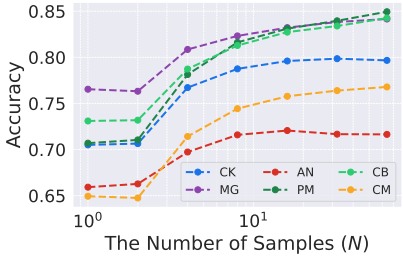

(f) One-stage CoT (Text) w/ Llama-8B

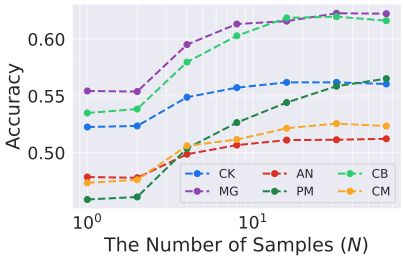

(g) Direct Answering (Text) w/ DeepSeek-8B

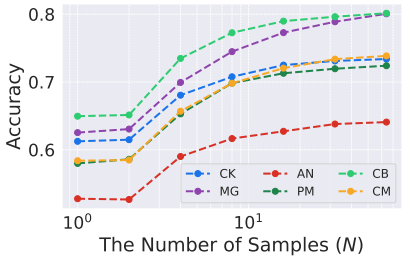

(h) One-stage CoT (Text) w/ DeepSeek-8B

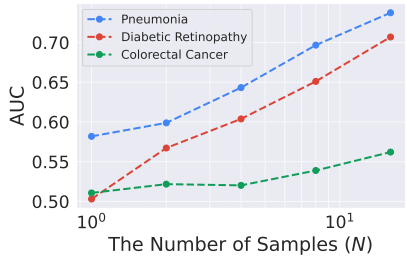

(i) Direct Answering (Vision) w/ Llama-11B-Vision

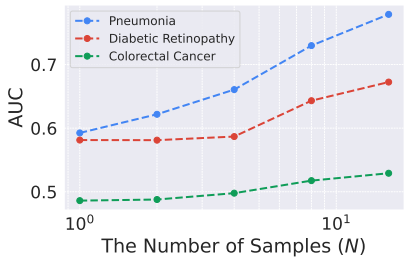

(j) One-stage CoT (Vision) w/ Llama-11B-Vision

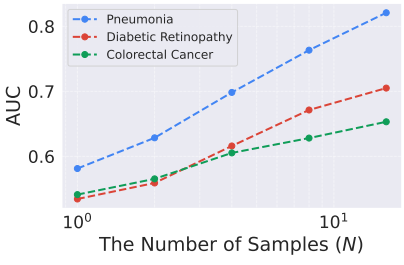

(k) Two-Stage Reasoning (Vision) w/ Llama-11B-Vision

Figure 4. A study examining the effect of sample size (N) in TTS setting. Increasing the sample size boosts performance across different datasets and inference methods, following a power law.